LARGE EDDY SIMULATION OF TURBULENT FLOW OVER A SPHERE USING AN IMMERSED BOUNDARY METHOD

DONGJOO KIM AND HAECHEON CHOI
School of Mechanical and Aerospace Engineering
Seoul National University, Seoul 151-742, Korea

Abstract. Large eddy simulation of turbulent flow over a sphere is conducted at two different Reynolds numbers (Re = 3700 and 10^4) based on the free-stream velocity and the sphere diameter, in order to investigate the flow characteristics over the sphere. The present numerical method is based on a newly developed immersed boundary method in a cylindrical coordinate (Kim *et al.* 2001). Also, a hybrid numerical method of eliminating 2-Δ waves in laminar accelerating flow region and also avoiding numerical dissipation in turbulent flow region is newly proposed for large eddy simulation of turbulent flow over a bluff body. At Re = 3700, the shear layer is elongated in the streamwise direction to form a cylindrical vortex sheet and its instability begins to appear at $x \approx 2d$. Also, the flow behind the sphere is nearly laminar at $x < d$ and contains few vortices. On the other hand, at Re = 10^4, the shear layer instability occurs right behind the sphere in the form of vortex tube and the flow becomes turbulent in the near wake. Therefore, at Re = 10^4, the size of the recirculation region is smaller and the wake recovers more quickly than at Re = 3700.

1. Introduction

Flow behind a sphere shows completely unsteady three-dimensional phenomena even at low Reynolds numbers (Sakamoto & Haniu 1990; Johnson & Patel 1999; Mittal 1999). Therefore, flow over a sphere has not been well understood as compared to that over a circular cylinder, even though the sphere geometry is simple. Previous studies on flow over a sphere have been mostly based on experimental methods, where vortical structures behind the sphere were presented using flow visualization and the high and low frequency characteristics in the shear layer, respectively, associated with the shear layer instability and the wake instability were investigated (Sakamoto

& Haniu 1990). When the Reynolds number exceeds about 800, the wake flow behind a sphere changes from laminar to turbulent flow. In recent years, a few numerical studies have been made on turbulent flow over a sphere (Tomboulides 1993; Constantinescu & Squires 2000). However, the detailed quantitative information on the turbulence statistics behind the sphere is still limited in the literature.

The objective of the present study is to investigate the characteristics of turbulent flow over a sphere using large eddy simulation at two different Reynolds numbers of 3700 and 10^4 based on the free-stream velocity u_∞ and the sphere diameter d.

2. Numerical Method

The present numerical method is based on a newly developed immersed boundary method in a cylindrical coordinate (Kim *et al.* 2001), where the sphere in the flow is treated as momentum forcing in the Navier-Stokes equations. Therefore, flow over the sphere can be easily handled with orthogonal (cylindrical) grids that do not coincide with the body surface. Numerical simulations are performed at two different Reynolds numbers of $\mathrm{Re} = u_\infty d/\nu = 3700$ and 10^4. The computational domain used is $-15d \leq x \leq 15d$, $0 \leq r \leq 15d$, $0 \leq \theta \leq 2\pi$, and the number of grid points is $577(x) \times 141(r) \times 40(\theta)$. Here, x, r and θ, respectively, denote the streamwise, radial and azimuthal directions. A Cartesian coordinate system (x, y, z) is also defined in order to present the drag and lift forces, where the y and z coordinates coincide with $\theta = 0^o$ and $\theta = 90^o$, respectively.

One of the important issues for large eddy simulation of turbulent flow over a bluff body at high Reynolds number is that the second-order central difference scheme produces serious dispersion errors for convection-dominated flow, and thus 2-Δ waves appear in the region of velocity acceleration (for example, at front surface of a sphere). To resolve this problem, two different approaches have been taken: One is to apply a filtering procedure which corresponds to adding numerical dissipation in an *ad hoc* manner, and the other is to use upwind or upwind-biased schemes. In these approaches, however, the numerical dissipation becomes larger than the dissipation from the subgrid-scale viscosity (Beaudan & Moin 1994).

In this study, we propose a hybrid approach for the spatial discretization of the convection terms for flow over a bluff body, where a high-order upwind scheme is used in the region of laminar accelerating flow and the second-order central difference scheme is used elsewhere. The diffusion terms are discretized with the second-order central difference scheme. With this approach, we can avoid possible contamination of solutions resulting from the application of the dissipative schemes to the whole flow field.

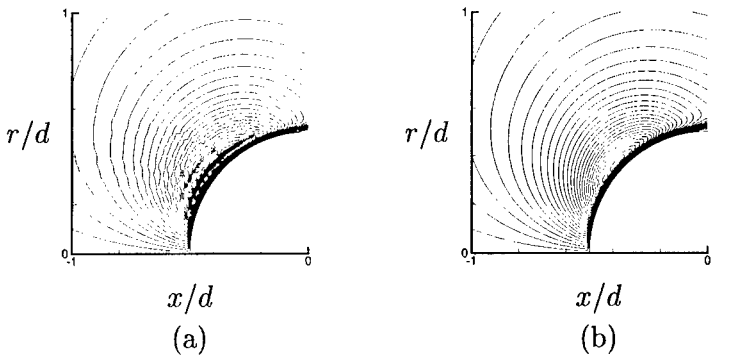

Figure 1. Contours of the instantaneous radial velocity in front of the sphere at Re = 3700: (a) second-order central difference scheme (CD); (b) hybrid scheme (CUDZ3+CD).

For the high-order upwind scheme, we use the third-order compact upwind scheme (CUDZ3) by Zhong (1998), which is stable and less dissipative than the straightforward compact upwind scheme using an upwind-biased grid stencil (Tolstykh 1994). For the flow over a sphere, we apply CUDZ3 to the laminar accelerating flow region ($x < 0$ and $r < d$).

Figure 1 shows the contours of the instantaneous radial velocity in front of the sphere at Re = 3700 using two different numerical schemes. Figure 1 (a) is obtained from the second-order central difference scheme (CD) applied to the whole flow field, whereas figure 1 (b) is from the hybrid scheme proposed in the present study. It is clear that the present hybrid scheme effectively removes the wiggles appeared in figure 1 (a). Therefore, all the following results presented in this paper are obtained using the hybrid scheme.

3. Results

The simulation results are summarized in table 1, where time-averaged drag coefficient ($\bar{C}_d$), base pressure coefficient ($\bar{C}_{p_b}$), separation angle ($\bar{\alpha}_s$), recirculation bubble size ($\bar{L}$), and Strouhal number (St) associated with the wake instability are presented together with experimental and computational data available. Here, LES and DES denote large eddy simulation and detached eddy simulation, respectively, and DES is a hybrid approach reducing to Reynolds-averaged Navier-Stokes (RANS) near the wall and LES away from the wall. The recirculation bubble size ($\bar{L}$) is the distance from the base of the sphere to the point where the time-averaged streamwise velocity is zero. The drag coefficient, base pressure coefficient, Strouhal number and separation angle are in reasonably good agreement with the

	Re	$\bar{C}_d$	$\bar{C}_{p_b}$	St	$\bar{\alpha}_s$	$\bar{L}/d$
Present	3700	0.36	-0.20	0.22	90^o	2.60
	10^4	0.40	-0.28	0.18	90^o	1.34
Exp^1	3700			0.22		
	4200		-0.23			
	10^4			0.16		
Exp^2	3700			0.21		
	10^4			0.18		
$Comp^1$ (LES)	10^4	0.393		0.195	$84^o - 86^o$	
(DES)	10^4	0.397		0.200	$84^o - 87^o$	

TABLE 1. Flow parameters of turbulent flows over a sphere. Exp^1, Kim & Durbin (1988); Exp^2, Sakamoto & Haniu (1990); $Comp^1$, Constantinescu & Squires (2000). Here, *Exp* and *Comp* denote experimental and computational studies, respectively.

previous results. $\bar{C}_d$ at Re = 3700 is smaller than that at Re = 10^4 in this study, which is closely related to the fact that the base pressure coefficient is larger at Re = 3700. It is interesting to note that even though the separation angle is the same for both Reynolds numbers, the recirculation bubble size at Re = 3700 is about twice that at Re = 10^4. This is closely associated with the characteristics of the separating shear layer, which is explained in the following.

Figure 2 shows the contours of the instantaneous azimuthal vorticity at Re = 3700 and 10^4 on the (x, y)-plane. At Re = 3700, the separating shear layer is elongated in the streamwise direction to form a cylindrical vortex sheet and its instability begins to appear at $x \approx 2d$. On the other hand, at Re = 10^4, the shear layer instability appears right behind the sphere. Note that the flow behind the sphere ($x < d$) at Re = 3700 contains few vortices, whereas at Re = 10^4 many small-scale vortices exist right behind the sphere. Therefore, at Re = 3700, the base pressure is higher and the drag coefficient is smaller than at Re = 10^4. Because strong vortical motion exists at $x \approx 2d$ for Re = 3700, the lift fluctuations are much smaller than those at Re = 10^4. Due to early onset of the shear layer instability and strong vortical motions in the near wake at Re = 10^4, the size of the recirculation region at Re = 10^4 is much smaller than that at Re = 3700.

For clear understanding of the three-dimensional structures in the near wake, vortical structures are drawn in two different ways in figure 3, where vortical surfaces are identified using the method of Jeong & Hussain (1995).

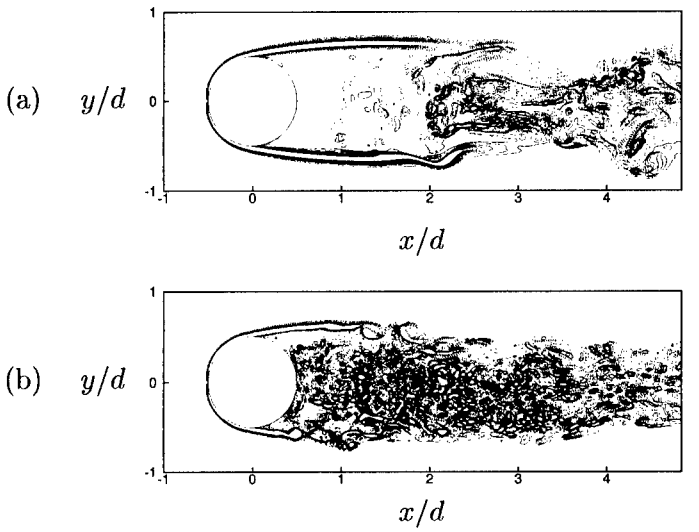

Figure 2. Contours of the instantaneous azimuthal vorticity: (a) Re = 3700; (b) Re = 10^4.

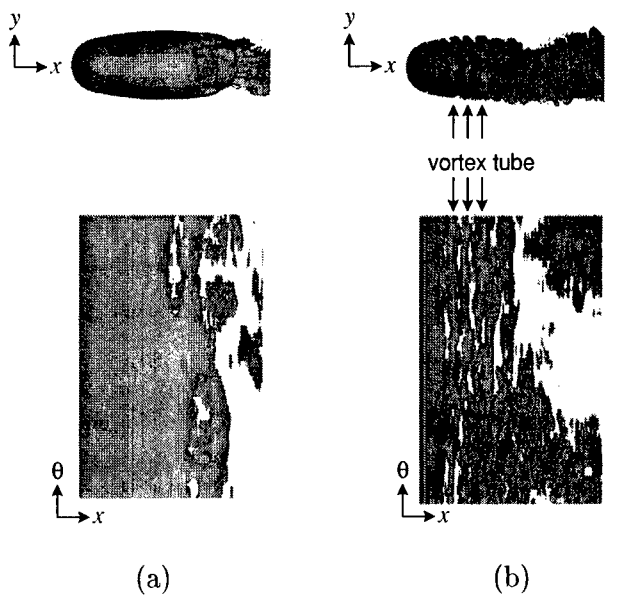

Figure 3. Vortical structure in the near wake: (a) Re = 3700; (b) Re = 10^4. In bottom figures, vortical surfaces are unfolded in the azimuthal direction.

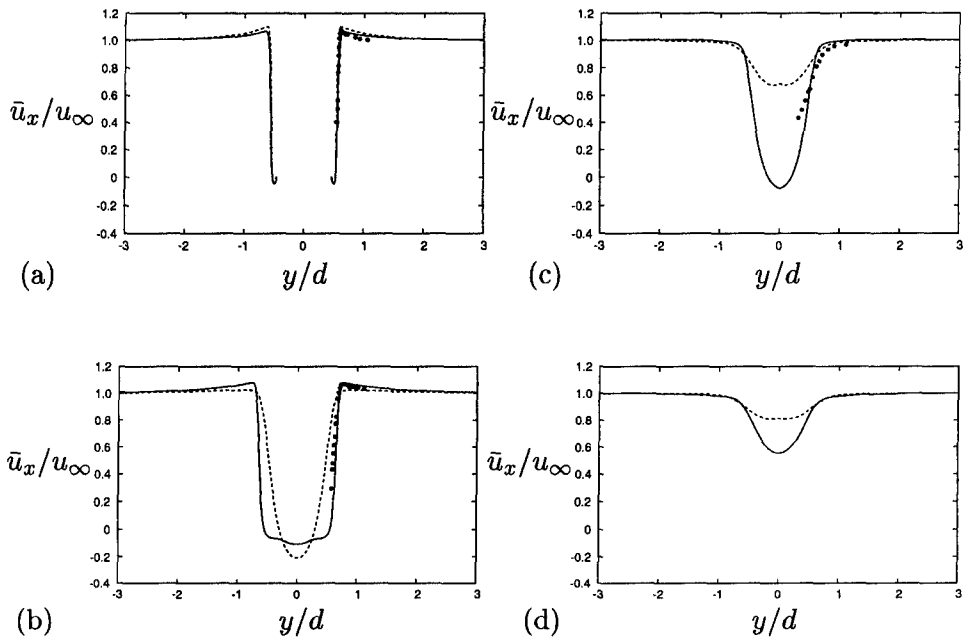

Figure 4. Streamwise velocity averaged in time and azimuthal direction: (a) $x/d = 0.2$; (b) $x/d = 1.6$; (c) $x/d = 3.0$; (d) $x/d = 4.0$. ———, Re = 3700 (present study); – – – –, Re = 10^4 (present study); •, Re = 3700 (Kim & Durbin 1988).

That is, top figures are the projection of vortical surfaces on the (x, y)-plane, whereas in bottom figures the vortical surfaces are unfolded in the azimuthal direction. At Re = 3700, the vortex sheet of the shear layer is broken away locally in the azimuthal direction. However, at Re = 10^4, the vortex sheet is broken away along the azimuthal direction to form vortex tubes. The term of vortex tube was defined by Sakamoto & Haniu (1990) as the cylindrical vortex shed from the vortex sheet separated from the sphere surface.

Figure 4 shows the streamwise velocities averaged in time and azimuthal direction at Re = 3700 and 10^4. The present results at Re = 3700 are in good agreement with those of single-wire measurements by Kim & Durbin (1988) at $x/d = 0.2$, 1.6 and 3.0. A difference is observed at $x = 3.0d$ because the measurement error of a single-wire probe becomes large near the end of the recirculation region, where the magnitude of the radial velocity is comparable to that of the streamwise velocity and thus the flow angle approaching the wire is not small. It is clear that the wake at Re = 10^4 recovers more quickly than that at Re = 3700.

Figures 5 shows the contours of the Reynolds shear stresses $(-\overline{u'_x u'_r}/u_\infty^2)$

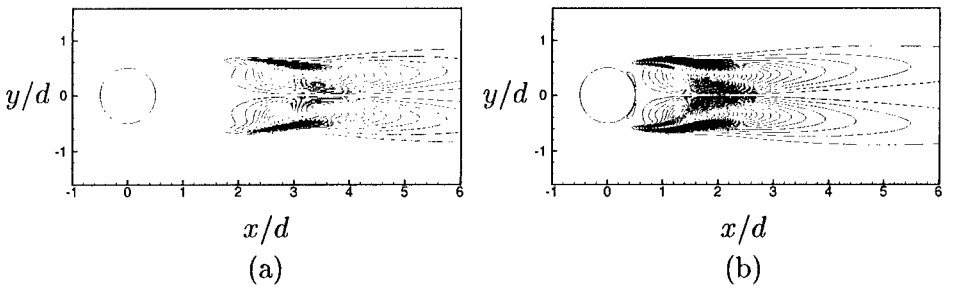

Figure 5. Contours of the Reynolds shear stress ($-\overline{u_x' u_r'}/u_\infty^2$) in the near wake: (a) Re = 3700; (b) Re = 10^4.

in the near wake at Re = 3700 and 10^4, where the shear stress is averaged in time and azimuthal direction. The Reynolds shear stress as well as the normal stresses (not shown here) are zero up to the separation point ($\alpha_s = 90^o$) for both Reynolds numbers, showing that the boundary layer flow before separation is laminar. It is clear that the transition of the wake to turbulence occurs right behind the sphere at Re = 10^4, whereas at Re = 3700 the transition occurs far downstream ($x \approx 2d$). This phenomenon is closely related to different onset of the shear layer instability between two Reynolds numbers.

4. Summary

In summary, the flow characteristics between two Reynolds numbers of Re = 3700 and 10^4 are quite different. At Re = 3700, the shear layer is elongated in the streamwise direction to form a cylindrical vortex sheet and its instability begins to appear at $x \approx 2d$. On the other hand, at Re = 10^4, the shear layer instability occurs right behind the sphere in the form of vortex tube and the flow becomes turbulent in the near wake. Note that the flow behind the sphere ($x < d$) at Re = 3700 is nearly laminar and contains few vortices. Therefore, at Re = 3700, the base pressure is higher and the drag coefficient is smaller than at Re = 10^4. Because the vortices exist at $x \simeq 2d$ for Re = 3700, the lift fluctuations are much smaller than those at Re = 10^4. At Re = 10^4, mixing in the near wake is much stronger than that at Re = 3700, and thus the wake recovers more quickly.

This work is supported by the Creative Research Initiatives of the Korean Ministry of Science and Technology.

References

BEAUDAN, P. & MOIN, P. 1994 Numerical experiments on the flow past a circular cylinder at sub-critical Reynolds number. *Report No. TF-62*, Department of Mechanical Engineering, Stanford University.

CONSTANTINESCU, G. S. & SQUIRES, K. D. 2000 LES and DES investigations of turbulent flow over a sphere. *AIAA paper 2000-0540.*

JEONG, J. & HUSSAIN, F. 1995 On the identification of a vortex. *J. Fluid Mech.* **285**, 69–94.

JOHNSON, T. A. & PATEL, V. C. 1999 Flow past a sphere up to a Reynolds number of 300. *J. Fluid Mech.* **378**, 19–70.

KIM, H. J. & DURBIN, P. A. 1988 Observations of the frequencies in a sphere wake and of drag increase by acoustic excitation. *Phys. Fluids* **31**, 3260–3265.

KIM, J., KIM, D. & CHOI, H. 2001 An immersed-boundary finite volume method for simulations of flow in complex geometries. *J. Comput. Phys.* **171**, 132–150.

MITTAL, R. 1999 Planar symmetry in the unsteady wake of a sphere. *AIAA J.* **37**, 388–390.

SAKAMOTO, H. & HANIU, H. 1990 A study on vortex shedding from spheres in a uniform flow. *J. Fluid Eng.* **112**, 386–392.

TOLSTYKH, A. I. 1994 High accuracy non-centered compact difference schemes for fluid dynamics applications. World Scientific, Singapore.

TOMBOULIDES, A. 1993 Direct and large-eddy simulation of wake flows: flow past a sphere. Ph.D. dissertation, Princeton University

ZHONG, X. 1998 High-order finite-difference schemes for numerical simulation of hypersonic boundary-layer transition. *J. Comput. Phys.* **144**, 662–709.